Structure and Morphology of an Intumescent Polypropylene Blend

X. Almeras,[1] N. Renaut,[1] C. Jama,[1] M. Le Bras,[1] A. Tóth,[2] S. Bourbigot,[1,3] Gy. Marosi,[4] F. Poutch[5]

[1]*Laboratoire des Procédés d'Élaboration des Revêtements Fonctionnels (PERF) UPRES EA 1040, ENSC-Lille, BP 108, 59652 Villeneuve d'Ascq Cedex, France*
[2]*Research Laboratory of Materials and Environmental Chemistry, Chemical Research Center, Hungarian Academy of Sciences, Budapest, Hungary*
[3]*École Nationale Supérieure des Arts et Industries Textiles (ENSAIT), Laboratoire GEMTEX, 9 rue de l'Ermitage, BP 30329, Roubaix Cedex 01, Roubaix, France*
[4]*Organic Chemistry Technology Department, Budapest University of Technology and Economics (BUTE), H-1111 Müegyetem rkp. 3, Budapest, Hungary*
[5]*Centre de Recherche et d'Etudes sur les Procédés d'Ignifugation des Matériaux (CREPIM), Rue Christophe Colomb, 62700, Bruay La Buissière, France*

Received 28 August 2003; accepted 30 January 2004
DOI 10.1002/app.20470
Published online in Wiley InterScience (www.interscience.wiley.com).

ABSTRACT: This article deals with the study of the efficiency of different compatibilizing agents in the intumescent polypropylene/polyamide-6/ammonium polyphosphate (PP/PA-6/APP) blend. The migration of additive was first investigated by X-ray photoelectron spectroscopy. The study showed that ethylene–butyl acrylate–maleic anhydride is not efficient in preventing the exudation of APP to the surface. However, ethylene vinyl acetate (EVA) prevented such a phenomenon. Second, the modifications in the blends were analyzed as a function of their compositions. Optical microscopy analysis showed that adding EVA to PP/PA-6/APP promoted a decrease in the size of PA-6 droplets. X-ray diffraction was used to characterize the effect of each component on the PP crystallinity. It was clearly shown that the crystallinity depends on the composition of the blend. © 2004 Wiley Periodicals, Inc. J Appl Polym Sci 93: 402–411, 2004

Key words: polypropylene (PP); intumescence; compatibility; morphology; crystal structures

INTRODUCTION

Polypropylene (PP) is widely used in many industrial applications because of its low cost and easy processing. However, PP burns very easily and dripping is observed during its combustion. The use of virgin PP is thus limited when flammability properties are required. Several approaches have been developed to increase its fire-resistant properties. Hornsby[1] reviewed the approach of using classical fillers in PP to increase its fire behavior. With classical filler, the main problem is the loading (typically between 40 and 60% in mass), which directly affects the mechanical properties of the polymer. Another problem is that the filler must be treated to increase its interfacial adhesion with the matrix.

Another solution to improve the fire-resistant properties of polymers is the use of intumescent additives.[2,3] Intumescent technology[4,5] has found a place in polymer science as a method of imparting flame retardancy to polymeric materials. On heating, fire retardant (FR) intumescent materials form a foamed cellular charred layer on their surfaces,[6,7] which protects the underlying materials from the action of heat flux and flame. The proposed mechanism[8] is based on the charred layer acting as a physical barrier, which retards heat and mass transfer between the gas and the condensed phase.

Generally, intumescent formulations contain three ingredients: an acidic source, a carbonization agent, and a blowing agent. The first generation of carbonization agents used in intumescent formulations for thermoplastics consists of polyols, such as pentaerythritol, mannitol, or sorbitol.[9–11] Problems include the migration/blooming of the additives, their water solubility, and their reaction with the acid source during the processing of the formulations. To solve this problem, polyamide 6 (PA-6) could be used as carbonization polymer.

Recent works have investigated the fire properties of intumescent PP blends.[3,12–14] It was shown that the addition of ammonium polyphosphate (APP) and polyamide 6 (PA-6) imparts desired fire properties to the blends. In particular, the limiting oxygen index (LOI) increases from 17 to 32 vol % O_2 when PP is blended with a combination of APP, PA-6, and ethyl-

Correspondence to: M. Le Bras (Michel.Le-Bras@ensc-lille.fr).

TABLE I
Fire and Mechanical Performance of PP and Intumescent Blends[a]

Sample	LOI (vol %)	HRR (kW/m^2)	Young modulus (MPa)	Elongation at Break (%)
PP	17 ± 1	1500 ± 150	1340 ± 150	14.5 ± 1
PP/PA-6/APP/EVA_{24},	33 ± 1	320 ± 30	1730 ± 190	9.6 ± 1
PP/PA-6/APP/EBuAMA	30 ± 1	400 ± 40	1520 ± 150	5.0 ± 1

[a] From Almeras et al.[13]

ene vinyl acetate (EVA). Moreover, O_2 consumption calorimetry shows a significant decrease in the peak of heat release rate (HRR) from 1500 kW/m^2 (virgin polymer[13–15]) to 320 kW/m^2 for the blend.[13] However, the stability of the APP/PA6 blends obtained by direct mixing of APP in molten PA-6 is low because of the poor compatibility of APP and PA-6; a migration of the mineral salt[16] occurs during solidification of molten blend versus time, and thus an interfacial agent is needed to prevent the exudation phenomenon.

EVA_x (where x is the percentage of vinyl acetate) are known to be efficient interfacial agents.[17,18] Moreover, incorporating APP/PA6 into EVA_x confers improved fire properties. Ethylene–butyl acrylate–maleic anhydride (EBuAMA) and EVA_x were used as interfacial agents in polyolefins in previous works.[19] Moreover, previous studies have shown that these interfacial agents[3–13] directly influence the fire properties. In particular, an acidity reinforcement of the intumescent char was proposed to explain the synergistic effect of EVA. Although the effect of interfacial agent on the fire properties was investigated, no investigation on the blend morphology was done.

The first part of this work is devoted to the determination of the surface composition of the blend by X-ray photoelectron spectroscopy (XPS). In a second part, the best formulation was chosen for investigation.

The fire performance and mechanical properties of PP/PA-6/APP blends (Table I)[13] were used to select a blend for further investigation, with respect to the XPS results.

Table I clearly shows that adding intumescent additives to PP induces a slight hardening of the polymeric material. Moreover, when the blend with either EVA_{24} or EBuAMA is compared with EVA, the blend presents the highest performance by considering each of the comparison criteria.

Both the additives and the morphology of the PP have a substantial influence on the properties. Indeed, PP is a polymorphic material[20] with a number of crystal modifications,[21] such as monoclinic (α), hexagonal (β), and triclinic (γ). The monoclinic (α) modifications occurs most frequently.[22–24] In the second part, the morphologies of PP/PA-6/APP/EVA and PP/PA-6/APP/EBuAMA are the principal topics of this study; more particularly, (1) the morphology of the blend is investigated by optical microscopy and scanning electron microscopy (SEM), and the crystallinity by X ray diffraction (XRD); and (2) the virgin polymer was investigated with respect to comparison of the changes induced by each component.

EXPERIMENTAL

Materials

The raw materials were polypropylene [PP; 3120 MN 1, grade 8 (230°C, 2.16 kg), MFI = 6, as pellets (appryl, ATOFINA Chemicals, Philadelphia, PA)], PA-6 (as pellets supplied by Nyltech, Manchester, NH), APP [AP 422: $(NH_4PO_3)_n$, $n \approx 700$; powder supplied by Clariant (Muttenz, Switzerland)], EBuAMA [ethylene (91.5 wt %)–butyl acrylate (5 wt %)–maleic anhydride (3.5 wt %), Lotader L-RAM 3200 as pellets; supplied by Elf Atochem (Paris, France)], and EVA_x (x from 8 to 24) supplied as pellets by Elf Atochem (EVATANE grades).

Processing

The melt-blending process was conducted using a Brabender DSE 25 intermeshing corotating twin-screw extruder (Brabender Instruments, South Hackensack, NJ) with five temperature zones. The thermal profile corresponding to each zone of the screw was set at 220 (amorcing zone), 225 (plastification zone), 230 (mixing zone), and 230°C. The rotational speed of the screws was set at 100 rpm. The polymers and additives were added in two steps. First, the polymers were introduced, then the APP was added just before the mixing zone. The different compositions of the blends are listed in Table II.

Sheets (3 mm thick) and tensile test samples were obtained by injection molding with an Allrounder 270S machine (Arburg Ltd., Warwick, UK). The thermal profile corresponding to each zone of the screw was set at 230, 235, 240, 245, and 250°C. The mold temperature was 50°C and the injection pressure and rate were 800 bar and 30 cm^3/s, respectively. The injected volume was 35 cm^3. The cooling time was 30 s.

TABLE II
Composition of the Tested Blends

PP (wt %)	PA-6 (wt %)	APP (wt %)	Compatibilizer	
			Type	(wt %)
100	—	—	—	—
70	30	—	—	—
70	25	—	EbuAMA	5
70	25	—	EVA 24	5
70	—	30	—	—
65	8.75	26.25	—	—
60	8.75	26.25	EbuAMA	5
60	8.75	26.25	EVA 8	5
60	8.75	26.25	EVA 19	5
60	8.75	26.25	EVA 24	5

Films (60 μm thick) were then obtained using a Darragon (Villecresnes, France) pressing machine at 230°C and at a pressure of 10^6 Pa for 3 min. Then the film was cooled to 40°C.

X ray photoelectron spectroscopy (XPS)

The XPS measurements were performed on an XSAM 800 apparatus (Kratos Analytical, Manchester, UK). The samples were mounted on a stainless steel sample holder by double-sided adhesive tape. Mg–$K_{\alpha 1,2}$ radiation was used. The spectra were recorded in fixed analyzer transmission mode. In particular, the wide-scan spectra were taken with 80-eV pass energy and 0.5-eV steps, whereas the detailed spectra were recorded with 40-eV pass energy and 0.1-eV steps.

The pressure in the analysis chamber was $<10^{-7}$ Pa. The spectra were referenced to the C1s line of the CH_x-type carbon [binding energy (BE) = 285 eV]. Data acquisition and processing were performed by the Kratos Vision 2000 software.

The peaks were resolved using peak analysis software (Peakfit, Jandel Scientific, San Rafael, CA) assuming a Gaussian line shape.

Optical microscopy

The morphology of the film was studied in the transmission mode by optical microscopy under polarized light using an Olympus (Osaka, Japan) BX60 microscope. Pictures were collected and analyzed using software from Microimage (Colombo, Sri Lanka).

Scanning electron microscopy

The specimens observed were fractured in liquid nitrogen and coated with a palladium–gold alloy to avoid charge by the electron beam. After coating the fracture surfaces, their observations were carried out with a JEOL 5300 scanning electron microscope (acceleration voltage, 20 kV; JEOL, Tokyo, Japan).

X-ray diffraction

XRD spectra were recorded by an automatic D5000 X-ray spectrometer (Siemens AG, Karlsruhe, Germany) using the Cu–$K_{\alpha 1,2}$ radiation and a nickel filter ($\lambda = 0.15406$ nm) in the range $12° < 2\theta < 55°$. These tests were carried out on sheets (1.6 mm thickness) with a rotation of the sheets to suppress structural orientation effects. DIFFRACT software (MM Research, Inc., Tucson, AZ) was used to subtract the $K_{\alpha 2}$ radiation component; to smooth the spectra; to subtract the amorphous zone; and, finally, to measure the intensity of the peaks. The Bragg and the Debye–Scherrer laws were used to determine the size of particles.[26,27] Moreover, XRD was used to determine the percentage of crystallinity for PP by the method described by Murthy et al.[28,29]

Differential scanning calorimetry

A DSC 92 thermal analysis system (SETARAM, Caluire, France) was used for thermal characterization. The temperature and the melting enthalpy were calibrated using standards (indium, zinc, bismuth, and lead) supplied by SETARAM. To study the PP crystallization, each sample was heated twice to 250°C at 5°C/min. Samples weighing about 10 mg were used. The crystallinity of PP (X_c) was calculated according to the following equation:

$$X_c = \frac{\Delta H_m m_c / m_p}{\Delta H_0} \quad (1)$$

where ΔH_m is the melting enthalpy measured in the second heating experiment, ΔH_0 is the theorical value of enthalpy of 100% crystalline PP ($\Delta H_0 = 207.1$ J/g)[27,45], m_c is the mass of the sample, and m_p is the mass of PP in the sample. The results are given in Table IV (DSC, [a]). However, another value is proposed for the theoretical melting enthalpy of 100% crystalline PP ($\Delta H_0 = 148$ J/g)[30] [see Table IV (DSC [b])].

RESULTS AND DISCUSSION

Surface composition

The surface compositions of different blends were analyzed using XPS.

The valence bands (VB) are very similar for each sample. This region is extremely "material sensitive," in the sense that usually substantial changes occur when passing from one material to another. The recorded VB spectra are similar to those published for PP,[32] where the bands between 4 and 12 eV are attributed to C2p-like electrons, whereas those between 12 and 22 eV are assigned to C2s-like ones. Thus, the

TABLE III
Surface Composition of Injected Blend

Sample	Experimental surface composition (atomic ratio)			Theorical surface composition (atomic ratio)		
	O/C	P/C	N/C	O/C	P/C	N/C
PP	0.038	0	0	0	0	0
PP/PA6/APP	0.018	0.003	0	0.18	0.058	0.072
PP/PA6/APP/EVA8%	0.008	0	0	0.19	0.058	0.072
PP/PA6/APPEVA19%	0.009	0	0	0.19	0.058	0.072
PP/PA6/APP/EVA24%	0.011	0	0	0.19	0.058	0.073
PP/PA6/APP/EBuAMA5%	0.044	0.003	0	0.19	0.058	0.073

recorded VB spectra suggest that the surface layer is composed primarily of PP. Surface composition data (atomic ratio results) are compiled in Table III.

It can be seen that the concentrations of O, N, and P at the surface do not correspond to theoretical surface composition data, thus confirming that different components are not uniformly distributed on the surface, given that the surface is rich in concentration of carbon atoms. This is attributed to the fact that a "skin effect" occurred when PP blends are injected.

No nitrogen was detected in any of the samples. This reflects the lack of significant amounts of the PA-6 char-forming agent in the surface layer of this series of samples:

- No phosphorus was detected in the surface of EVA-containing samples. This could be explained by the fact that APP is embedded in the polymer matrix in these samples.
- Very small amounts (~ 0.3 atomic %) of P could be detected in the surface layers of samples PP/PA6/APP and PP/PA6/APP/EBuAMA5%. The absence of N is very surprising, especially with the presence of P. Indeed, a previous study has shown no modification of APP after one extrusion and injection molding.[31]
- Oxygen content is very low, varying between about 1 and 4 atomic %. The presence of small amounts of oxygen is usual at the surface of polyolefins. Its origin is not known exactly, but probably can be connected to surface oxidation occurring during processing. [The binding energy of the O1s electrons is 532 ± 0.1 eV in each sample. This is closer to the BE of oxygen in the carbonyl group (about 532.3 eV) than to that in ether and/or alcohol type groups (~ 533 eV).][32]

The oxygen content at the surface is the highest for the blend with EBuAMA. Two reasons could explain this observation. The first concerns the presence of phosphorous at the surface attributed to the migration of APP. APP has three oxygens for one phosphorous, which means that 0.9% is the highest concentration of oxygen linked to phosphorous in APP at the surface. However, the increase in the oxygen amount with EBuAMA is more important and the amount of phosphorous compound (APP) constitutes one reason, although the explanation is insufficient to understand why the amount of oxygen/carbon increases from 0.011 to 0.044%. The second could be a slight degradation of the material during the process, especially of EBuAMA inducing an increase in the oxidation.

The difference of oxygen concentration between the PP/PA-6/APP and the blend with EVA_{24} is 0.07; thus, considering the amount of oxygen in APP, there is no modification of the oxidation on the blend surface between PP/PA-6/APP and PP/PA-6/APP/EVA_{24}. The addition of EVA_{24} apparently should not modify the oxidation aspect on the surface during the processing.

The C1s spectra are plotted in Figure 1. All peaks for each system are superposed. For all systems, one peak is distinguished around 285 eV. With full width at half maximum of 1.8 eV, it is ascribed to the contribution of C—H and C—C in the aliphatic species. No oxidized carbon species are present (i.e., C—O and C═O),

TABLE IV
Interreticular Distance and Crystallite Size in the PP Blends

Sample	d_{110} (nm)	d_{040} (nm)	Crystallinity (%) XRD	Crystallinity (%) DSC [a]	Crystallinity (%) DSC	L (nm)
PP	0.624	0.520	61	42	58	15.4
PP/APP	0.624	0.520	49	39	55	30.6
PP/PA-6/APP	0.624	0.520	54	47	66	18.3
PP/PA-6/APP/EVA_{24}	0.624	0.520	65	50	71	35.8

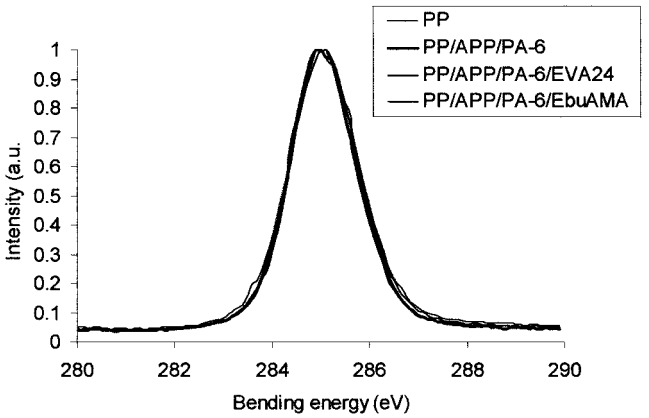

Figure 1 C1s spectra of the different PP blends.

which is probably attributable to the small oxygen concentration.

The XPS study has shown that the same results were obtained without interfacial agent or with EBuAMA, whereas there was no phosphorus content at the surface with EVA_x. This clearly proves that the two interfacial agents do not act in the same way.

However, similar results are obtained irrespective of the type of EVA used; thus the study will concern the investigation of only EVA_{24}. This choice was made because of the fire properties and the mechanical properties.[13]

Morphology

Images of different blends are presented and compared to investigate the effect of each component on the morphology.

Figure 2 shows the presence of spherulites[15] with a diameter of about 60 μm. Norton and Keller[33] studied the spherulitic morphology. More particularly, they showed that the spherulites present different optical orientations in function of their orientations and crystallized structures. Considering the images proposed by Norton and Keller,[33] the similarities of the results suggest that these spherulites are a "mixed" spherulite type. These spherulites exhibit random distributions of positively and negatively birefringent regions. Moreover, the presence of spherulites verifies that the film is anisotropic. The dark portion could correspond either to the joints between the spherulites or to some defects of the film.

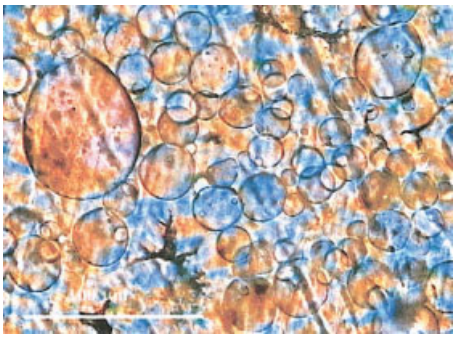

Figure 3 PP/PA-6 film under polarized light.

Figure 3 depicts a PP/PA-6 blend, showing the presence of a large crystallized phase in red evidenced by the blue color to the polarized light. The spherical nodules are probably PA-6.[34] This distribution is typical of an uncompatibilized alloy. Moreover, the size distribution of the PA-6 droplets ranges from 5 to 60 μm. Some spherulites are visible in the background. PA-6 does not prevent spherulite formation, although their dimensions decrease. It is possible that this could result from the stress induced during the cooling. The presence of spherulites proves that the film is inhomogeneous.

Figure 4 shows the EVA effect on the PP/PA-6 blend morphology. Thus adding 5 wt % of EVA to the incompatible blends of PP/PA-6 increased the PA-6 dispersion, with a reduction in the size of the domains to 5 μm. The same effect was previously observed when PP with grafted maleic anhydride was added to the PP/PA6 blend.[35] EVA acts as an interfacial agent that induces a decrease in the interfacial tension between PP and PA-6. However, spherulites are no longer visible. The blend is an isotrope.

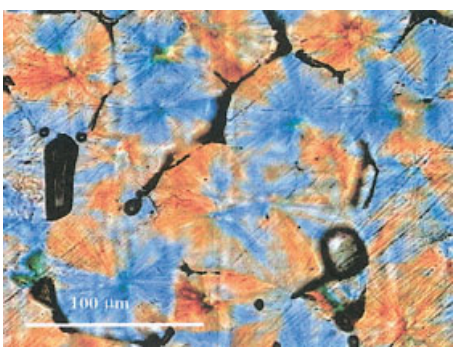

Figure 2 PP film under polarized light.

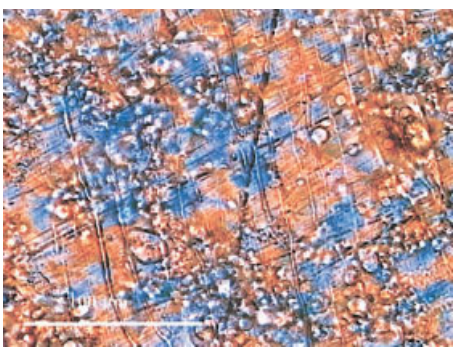

Figure 4 PP/PA-6/EVA_{24} film under polarized light.

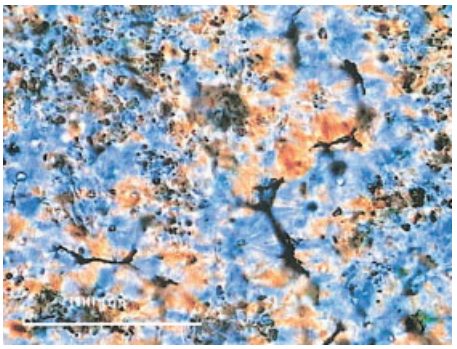

Figure 5 PP/APP film under polarized light.

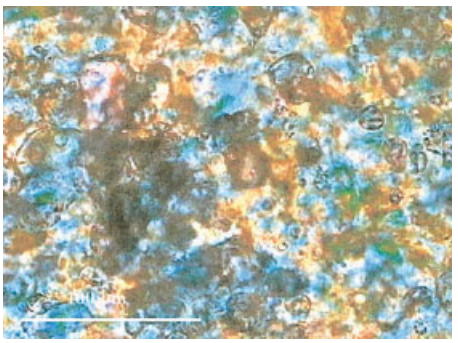

Figure 7 PP/PA-6/APP/EVA_{24} film under polarized light.

Figure 5 provides evidence of the effect of APP on PP morphology. Thus, this film presents a similar aspect to the virgin polymer: in particular, the polarized light revealed the presence of spherulites. Moreover, particles between the spherulites are probably APP grains. The last point concerns the spherulite aspect: it is the same as in the virgin PP, although the size of the spherulites decreases.

The effect of the addition of PA-6/APP on the PP blend morphology is shown in Figure 6. In the PP, 9 wt % of PA-6 was added and 25 wt % of APP. However, some droplets, visible in Figure 6, are similar to the droplets in the PP/PA-6 blend with a constant diameter ($\sim$ 5 μm). The dark portion is probably attributable to the APP grain, as observed in PP/APP blend. In the background, the PP part is observable. Some spherulites of 10 μm are visible.

The composition of the blend depicted in Figure 7 is similar to the blend shown in Figure 6, but 5 wt % of PP is substituted by EVA_{24}. In the background, the PP phase is observable and, apparently, no spherulites are visible. This confirms the observation from Figure 4, which was that EVA prevents the formation of spherulites. The dark portion is assigned to the APP, as in the image without EVA_{24}. However, droplets of PA-6 are visible but their size is less than 5 μm. However, no droplets of EVA are visible in the blend, and it is thus presumed that EVA is not dispersed in the matrix, like PA-6, but it could be located near the APP, as proposed by Le Bras et al.[16] in the PA-6/APP blend. Moreover, adding EVA leads to an improvement of the distribution of APP.

According to Figure 8, the PA-6 droplets are visible in the blend, but their size is about 2 μm. The white portion is probably some APP particles. The image confirms the first observation obtained by optical microscopy with the presence of small droplets of PA-6 in the matrix.

Because the microscopy shows some difference in the morphology, the structure was investigated by XRD and DSC.

The X ray diffraction spectra of the PP, PP/APP, PP/PA-6/APP, and PP/PA-6/APP/EVA_{24} are shown in Figures 9, 10, 11, and 12, respectively. The XRD study verifies that the polymeric materials studied are both amorphous and crystalline and that APP is a crystalline compound. The PP spectrum presents five diffraction rays assigned to the (110), (040), and (120) planes of the α-allotropic variety that presents a monoclinic structure.[22,36]

We were then able to determine the percentage of crystallinity for PP by the method described by Mur-

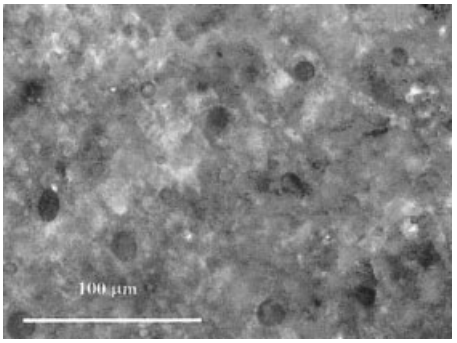

Figure 6 PP/PA-6/APP film under polarized light.

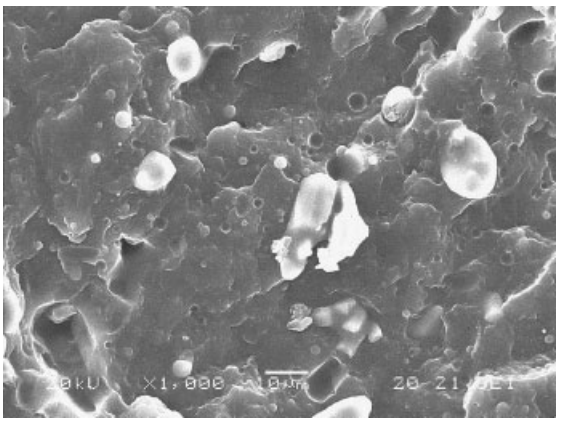

Figure 8 Morphology of PP/PA-6/APP/EVA_{24} blend by SEM at 20 kV(*1000).

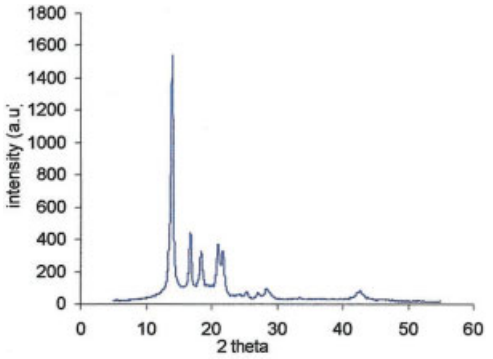

Figure 9 XRD spectrum of PP.

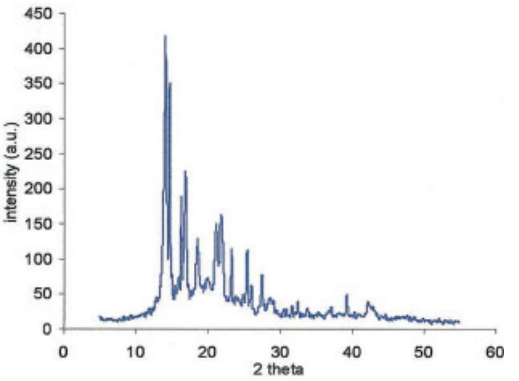

Figure 11 XRD of PP/PA-6/APP.

thy and Minor[28], in each blend (presented in Table IV), and then to compare these data to the DSC results.

APP exists under different crystalline forms[37]: form II is orthorhombic, form IV is monoclinic, and form V is orthorhombic. APP is commercialized under two crystalline forms, type I and type II.[38] The XRD spectrum of the form II of APP is well known.[16] The diffraction rays of APP are visible irrespective of the blend.

The PP/APP spectrum corresponds to the sum of the PP and APP spectra. However, some modifications appear concerning the peak intensities, showing a modification in the crystallinity. This clearly shows the absence of interaction between the PP and the APP. Moreover, as previously observed by ^{31}P-NMR,[31] there is no modification of the APP during the process.

The addition of 9 wt % of PA-6 does not induce any modification compared to the PP/APP spectrum data. The PA-6 spectrum presents two diffraction rays[29] assigned to the (200) and (002, 202) planes of the allotropic variety α of PA-6, respectively, for $d = 0.441$ nm ($2\theta = 20°$) and $d = 0.375$ nm ($2\theta = 23.7°$).[29] These two peaks are very weak. Moreover, these two peaks correspond to two diffraction rays of APP. Thus these peaks are probably the addition of the contribution of the two materials, but do not identify the PA-6 structure in the blend.

Concerning the addition of EVA in the blend, there is no major modification of the blend spectrum. The EVA XRD spectrum was previously published.[16] The EVA spectrum is distinguished by a intense ray ($d = 0.415$ nm; i.e., $2\theta = 21.4°$) and a smaller one ($d = 0.378$ nm; i.e., $2\theta = 23.5°$). These rays are identified again on the spectra of the blends.

These two peaks appear at the same 2θ as that of PP ($2\theta = 21.4°$) and PA-6 ($2\theta = 23.5°$) and cannot be distinguished on the spectrum. On the spectrum of the PP/PA-6/APP/EVA blend, no peak appears at $2\theta = 23.5°$, which suggests that the addition of EVA in the blend might modify the crystallinity of PA-6.

An additional diffraction peak appears at $2\theta = 15.16$, which may be assigned to mono-ammonium orthophosphate ($NH_4H_2PO_4$).[28,29] It was previously observed that this species forms with organic phosphates with short P—O—P chains, during compounding of intumescent polymeric formulations, by the reaction of APP with a carbonizing agent (polyol, starch[39]). These results are in opposition with the ^{31}P-NMR results.[37]

Moreover, the breaking of the APP chain under the combined action of heat and shear stress may be assumed with a subsequent reaction with water dissolved in PA-6 (1 to 6 wt % relative to PA-6, depend-

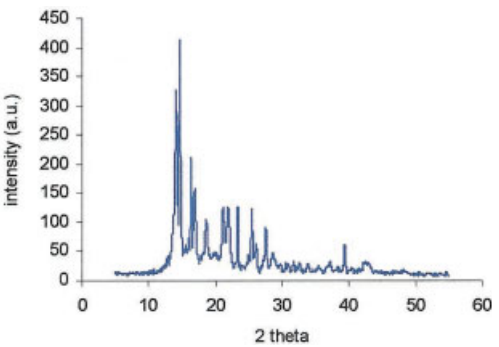

Figure 10 XRD spectrum of PP/APP.

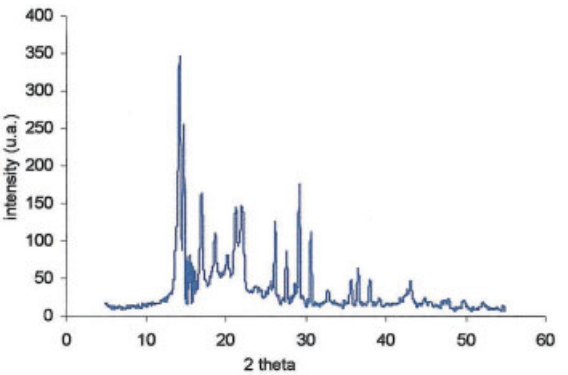

Figure 12 XRD spectrum of PP/PA-6/APPEVA$_{24}$.

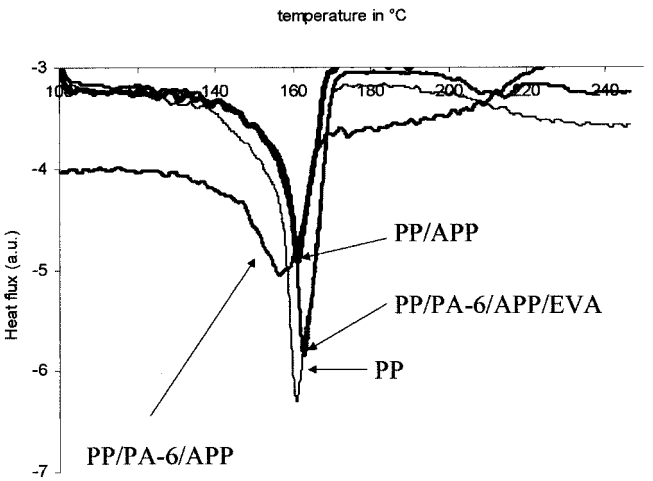

Figure 13 DSC endotherms (50°C/min).

ing on the laboratory conditions) and/or the reaction between the polyphosphate and PA-6[17,18] in the blending experimental conditions.

Furthermore, XRD is useful for determining the interlamellar distance (d-spacing) and the size (L) of the crystallites constituting the spherulites. The calculated crystallite size for PP in all the blends is indicated in Table IV, with the interreticular distance obtained with Bragg's law. Table IV shows that the interreticular distances d_{110} and d_{040} of PP do not change versus the blend composition, so it may be assumed that the additives are not inserted in the PP crystalline phases, as suggested by optical microscopy.

The value of L depends on the blend composition. First, the determined value for the crystallite in PP is in agreement with the results obtained by Monasse,[43] who found that the lamella size of the crystallite in the spherulite ranges between 10 and 50 nm, whereas the same dimensions are determined for the virgin polymer and for the PP/PA-6/APP blend, twice obtained for the PP/APP and PP/PA-6/APP/EVA_{24} blend.

The percentage of the crystalline form (computed using the protocol of Murthy and Minor[28]), very close to that of virgin PP, seems to imply that the semicrystalline state of the PP is preserved irrespective of the blend. A slight difference in the crystallinity was observed between the PP/PA-6/APP/EVA_{24} and the PP/APP by XRD. The crystallinity depends on (1) the integration of the spectra, to subtract the amorphous part; and (2) the precision of the measure of the contributions of APP and the other additive. The amount of crystallinity is very high, which is probably attributed to an overevaluation. An incertitude of 10% could be estimated. By DSC, the measure is probably more precise, although the difference between the limits is only 10%.

The additives apparently do not affect the crystal structure of PP. Similar results were first observed as reported in the literature.[40] However, this depends on the fillers. Indeed, in the crystallization of conventional PP grades, essentially the α-modification is formed, which may be accompanied by a lower or higher amount of β-modifications as a function of the cooling condition. Moreover, the β-modifications could be the consequence of the presence of β-nucleating agent such as fillers. Furthermore, although it has been suggested that uncoated fillers can induce formation of the PP β-phase,[41,42] the evolution of the XRD spectra has clearly shown that APP is not a β-nucleating agent and, further, has no major effect on the crystallinity of the PP.

The absence of effect of APP on the crystallinity was first observed in the EVA/PA-6 blend.[16] Perhaps the APP chains are too long to act as a nucleating agent.

However, DSC analysis was useful, not only in characterizing the amount of crystallinity of PP but also in studying the PA-6 form.

The DSC melting curves of PP blends (Fig. 13), at a heating rate of 5°C/min, show a difference in the melting peak of PP. For the PP/PA-6/APP blend, a wide peak of fusion is observed, whereas for the other blends, a sharp peak is observed. Moreover, the melting peak attributed to the PA-6 is observable in the PP/PA-6/APP/EVA blend, proving that PA-6 and PP are not compatible. The melting temperature of PP was determined with DSC curves, and the data are presented in Table V.

The melting point of each blend is similar, which confirms that the crystallinity type of PP in each blend does not evolve, as suggested by XRD.

DISCUSSION

Adding APP and PA-6 with or without interfacial agent has a different effect on the blend structure. Some exudation problems are observed without interfacial agent. Adding EVA prevents this phenomenon and modifies the morphology of the blend. Indeed, a decrease in the size of the PA-6 droplets is evidenced when EVA is added. The decrease in the dimension of the dispersed phase was first observed in different polymer blends.[45–48] These studies reported an efficiency of the compatibilizing agent, which reduces

TABLE V
Melting Temperature of the PP in the Different Studied Blends Determined by DSC at 5°C/min under N_2

Material	Melting point of PP (°C)
PP	161 ± 2
PP/APP	161 ± 2
PP/PA-6/APP	158 ± 2
PP/PA-6/APP/EVA_{24}	162 ± 2

interfacial tension, and an increase in mechanical properties.

A surface morphology study conducted by Le Bras et al.[16] showed that EVA_8 encapsulated APP, thus preventing APP exudation. However, in the PP/APP/PA-6/EVA blend, EVA is not visible. Moreover, addition of EVA modifies the PA-6 structure, as shown by the XRD spectrum; indeed, no diffraction peak attributed to PA-6 was observed. We thus suppose that EVA_{24} acts between APP and PA-6 and not between PP and PA-6 in PP/PA-6/APP blend.

Another point is that the crystallinity and the additives affected the mechanical properties. Indeed, a high percentage of crystallinity would induce a decrease in the chain mobility and the additives could act as a weak point because of the absence of sizing agent.[15]

Considering the blend aspect and the ^{31}P-NMR results,[32] no degradation occurs during the process. However, the presence of mono-ammonium orthophosphate was observed using XRD. Moreover, the addition of APP does not modify the crystallinity of the PP. Indeed, the α-monoclinic structure was maintained and the crystallinity ratio was kept constant. APP does not play the role of a β-nucleating agent.

CONCLUSIONS

As previously shown, adding APP/PA-6 to PP induces good fire properties, although the use of an interfacial agent is required. This work shows that adding PA-6/APP with an interfacial agent in PP leads to different behavior of the additive. Some exudation phenomena appear, or not; that is, APP is maintained in the core of injected samples. EBuAMA is not efficient for compatibilizing the blend with APP. For EVA_{24}, the behavior is different.

This study clearly shows the efficiency of EVA_{24} in preventing exudation. Moreover, it promotes a decrease in the size of PA-6 droplets, leading to the creation of an interphase at the PA-6/APP interface. This interphase imparts good mechanical properties and has a synergistic effect on the fire properties. The properties of the blend are closely dependent on its morphology. Furthermore, because no sizing agent is used with APP, there is probably the potential of increasing the mechanical properties by increasing the interactions between PP and APP.

References

1. Hornsby, P. R. Int Mater Rev 2001, 46, 199.
2. Montaudo, G.; Scamporino, E.; Vitalini, D. J Polym Sci Part A: Polym Chem 1983, 21, 3361.
3. Le Bras, M.; Bourbigot, S. In: Title of Series; Nelson, G. L.; Wilkie, C. A., Eds.; Symposium Series No. 797; ACS Polymeric Materials: Science and Engineering Division (PMSE); American Chemical Society: Washington, DC, 2001; Chapter 11, p. 797.
4. Tramm, H. L. U.S. Pat. 2,106,938, 1938.
5. Vandersall, H. L. J. Fire Flammability 1971, 2, 97.
6. Montaudo, G.; Scamporino, E.; Vitalini, D. J Polym Sci Part A: Polym Chem 1983, 21, 3361.
7. Camino, G.; Costa; Trossarelli. Polym Degrad Stab 1984, 7, 25.
8. Bourbigot, S.; Le Bras, M.; Delobel, R. J Fire Sci 1995, 13, 3.
9. Delobel, R.; Le Bras, M.; Ouassou, N.; Alistiqa, F. J Fire Sci 1990, 8, 85.
10. Le Bras, M.; Bourbigot, S.; Le Tallec, Y.; Laureyns, J. Polym Degrad Stab 1997, 56, 11.
11. Le Bras, M.; Bourbigot, S. In: Polypropylene: An A–Z Reference; Karger-Kocsis, J., Ed.; Kluwer Academic: Dordrecht, The Netherlands, 1999; p. 357.
12. Bourbigot, S.; Le Bras, M. In: International Plastics Flammability Handbook; Troitzsch, J.; Bourbigot, S.; Le Bras, M., Eds.; Hanser: New York, 2004; Chapter 5.
13. Almeras, X.; Dabrowski, F.; Le Bras, M.; Poutch, F.; Bourbigot, S.; Marosi, G.; Anna, P. Polym Degrad Stab 2002, 77, 305.
14. Almeras, X.; Dabrowski, F.; Le Bras, M.; Poutch, F.; Bourbigot, S.; Marosi, G.; Anna, P. Polym Degrad Stab 2002, 77, 314.
15. Shields, T. J.; Zhang, J. In: Polypropylene: An A–Z Reference; Karger-Kocsis, J., Ed.; Kluwer Academic: Dordrecht, The Netherlands, 1999; p. 247.
16. Le Bras, M.; Bourbigot, S.; Felix, E.; Pouille, F.; Siat, C.; Traisnel, M. Polymer 2000, 41, 5283.
17. Levchik, S. V.; Costa, L.; Camino, G. Polym Degrad Stab 1992, 36, 229.
18. Levchik, S. V.; Costa, L.; Camino, G.; Levchik, G. F. Fire Mater 1995, 19, 1.
19. Bourbigot, S.; Le Bras, M.; Siat, C. In: Recent Advances in Flame Retardancy of Polymeric Materials, Vol. 7; Lewin, M., Ed.; BCC Publishers: Norwalk, CT, 1997; p. 146.
20. Varga, J. J Mater Sci 1992, 27, 2557.
21. Turner-Jones, A.; Aizlewood, J. M.; Beckett, D. R. Makromol Chem 1964, 75, 134.
22. Natta, G.; Corradini, P.; Cesari, M. Atti Accad Nazl Lincei Rend Classe Sci Fis Mat Nat 1956, 21, 365.
23. Keith, H. D.; Padden, F. J.; Walter, N. M.; Wyckoff, H. W. J Appl Phys 1959, 30, 1485.
24. Wilchinsky, Z. W. J Appl Phys 1960, 31, 1969.
25. Morrow, D. R. J Macromol Sci Phys 1969, B3, 53.
26. Lemaitre, J. L.; Goving Menon, P.; Delannay, F. Heterogeneous Catalyst, Vol. 15; Delannay, F., Ed.; Marcel Dekker: New York, 1984; p. 299.
27. Wunderlich, B. Thermal Analysis; Academic Press: New York, 1990; p. 418.
28. Murthy, N. S.; Minor, H. Polymer 1990, 31, 996.
29. Murthy, N. S. Polym Commun 1991, 32, 301.
30. Varga, J.; Ehrenstein, G. W. In: Beta-Modification of Isotactic Polypropylene (Shields, T. J.; Zhang, J., Eds.); Polypropylene: An A–Z Reference; Karger-Kocsis, J., Ed.; Kluwer Academic: Dordrecht, The Netherlands, 1999; p. 247.
31. Almeras, X.; Le Bras, M,; Hornsby, P.; Bourbigot, S.; Marosi, G.; Anna, P.; Delobel, R. Polym Recycl, to appear.
32. Beamson, G.; Briggs, D. High Resolution XPS of Organic Polymers: The Scienta ESCA300 Database; Wiley: Chichester, UK, 1992.
33. Norton, D. R.; Keller, A. Polymer 1985, 26, 704.
34. Shi, D.; Ke, Z.; Yang, J.; Gao, Y.; Wu, J.; Yin, J. Macromolecules 2002, 35, 8005.
35. Roeder, J.; Oliveira, R. V. B.; Gonçalves, M. C.; Soldi, V.; Pires, A. T. N. Polym Test 2002, 21, 815.
36. Mencik, Z. J Macromol Sci Phys 1972, B6, 101.
37. Camino, G.; Luda, M. P. In: Mechanistic Study on Intumescence; Le Bras, M.; Camino, G.; Bourbigot, S.; Delobel, R., Eds.; Fire

Retardancy of Polymers: The Use of Intumescence; The Royal Chemical Society: Cambridge, UK, 1998; pp. 48–63.
38. Duquesne, S. Ph.D. Thesis, Université des Sciences et Technologie de Lille, France, 2001.
39. JCPDS–International Centre for Diffraction Data. File number 27-0062.
40. Padden, F. J.; Keith, H. D. J Appl Phys 1959, 30, 1479.
41. Velasco, J. I.; Morhain, C.; Martinez, A. B.; Rodriguez-Perez, M. A.; De Saja, J. A. Polymer 2002, 43, 6805.
42. Shi, G.; Chu, F.; Zhou, G.; Han, Z. Makromol Chem 1989, 190, 907.
43. Monasse, B. Ph.D. Thesis, Ecole des Mines, Paris, 1982.
44. Seyvet, O.; Navard, P. J Appl Polym Sci 2000, 78, 1130.
45. Greco, R.; Malincinico, M.; Martuscelli, E.; Ragosta, G.; Scarinzi, G. Polymer 1987, 28, 1185.
46. Park, S. J.; Kim, B. K.; Jeong, H. M. Eur Polym Mater 1990, 26, 131.
47. Ide, F.; Hasegawa, A. J Appl Polym Sci 1974, 18, 1974.
48. Willis, J. M.; Caldas, V.; Favis, D. B. J Mater Sci 1991, 26, 4742.